



Oxygen surface exchange and diffusion studies of $\text{La}_2\text{Mo}_2\text{O}_9$ in different exchange atmospheres

J. Liu^a, R.J. Chater^a, R.J.H. Morris^b, S.J. Skinner^{a,*}

^a Department of Materials, Imperial College London, Prince Consort Road, London SW7 2BP, UK

^b Department of Physics, University of Warwick, Gibbet Hill Road, Coventry, CV4 7AL, UK

ARTICLE INFO

Article history:

Received 3 October 2010

Received in revised form 11 February 2011

Accepted 18 February 2011

Available online 21 March 2011

Keywords:

$\text{La}_2\text{Mo}_2\text{O}_9$

Oxygen diffusion

Isotopic exchange

SIMS depth profiling

Water vapor

Ionic conductivity

ABSTRACT

A combination of ^{18}O tracer isotopic exchange and Secondary Ion Mass Spectrometry (SIMS) measurements was applied to obtain oxygen surface exchange and diffusion coefficients of $\text{La}_2\text{Mo}_2\text{O}_9$. The isotopic exchange was conducted in dry ($^{18}\text{O}_2$) and wet (H_2^{18}O) exchange atmospheres respectively with the advantages and disadvantages of each exchange discussed. A decrease in the oxygen diffusion coefficients was observed for the wet exchange method which was accompanied by an increase in the oxygen diffusion activation energy, indicating that the humidified and dry atmospheres affect the oxygen transport differently. Changes in the surface exchange coefficients at the phase transition temperature were observed suggesting a different rate-limiting step in the oxygen exchange and diffusion processes. The oxygen diffusivity was correlated to the ionic conductivity using the Nernst–Einstein relation from which the concentration of mobile oxygen ions was estimated to be 5 per unit cell. The result is consistent for both the calculated conductivity from diffusion coefficients and the measured values from the AC impedance spectroscopy.

© 2011 Elsevier B.V. All rights reserved.

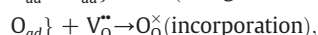
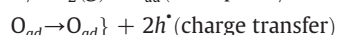
1. Introduction

As a fast oxide ion conductor, $\text{La}_2\text{Mo}_2\text{O}_9$ has attracted significant interest as an alternative electrolyte since its introduction by Lacorre [1] due to its excellent ionic conductivity at high temperature which is comparable to the commercialized yttria stabilized zirconia (YSZ) and gadolinium doped ceria (CGO). To date, there are a number of studies detailing its crystal structure, electrochemical properties and the effects of rare-earth substitutions on both the La and Mo sites to stabilize the phase transition that occurs at about 570 °C [2–4]. However, there are few oxygen diffusion studies of this material because of the difficulties with the oxygen exchange process at the surface. The only work published on the oxygen exchange and diffusion measurement of $\text{La}_2\text{Mo}_2\text{O}_9$ was carried out in a wet atmosphere (labeled H_2^{18}O) because of the restricted oxygen surface exchange in $^{18}\text{O}_2$ gas due to the low electron availability of $\text{La}_2\text{Mo}_2\text{O}_9$ [5].

The measurement of oxygen diffusion coefficients, which involves $^{18}\text{O}/^{16}\text{O}$ isotopic exchange and secondary ion mass spectrometry (SIMS), has been used to investigate oxygen transport properties for many electro-ceramic materials [6,7]. Initially, the sample is annealed in an oxygen tracer environment and then a SIMS depth profile/line scan technique is employed to obtain the oxygen diffusion profile from which the diffusion coefficient (D^*) and the surface exchange

coefficient (k) can be determined, as described in previous reports [8]. The obtained oxygen diffusion coefficient describes the oxygen ion transport properties within a material, while the oxygen surface exchange coefficient details the surface exchange kinetics.

The following steps have been suggested as the mechanism for the oxygen incorporation process in electro-ceramics: [9].

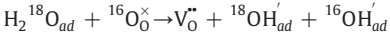


where the surface reaction is governed by the interaction of gaseous oxygen molecules, oxygen vacancies, and electron holes in the material. Which of these three is the rate-determining step is still under investigation. Manning et al. [8] reported that for ceria, the charge transfer step is rate determining because the activation energy of the surface exchange process is half that of the electronic band gap of the material. However, after comparing the surface exchange coefficients of two materials with different electron concentrations, Horita et al. [10] suggested surface adsorption/dissociation of oxygen as the rate-determining step. It appears that the situation may vary for different materials, but one thing is certain, the formation of $\text{O}_{\text{ad}}^{\bullet}$ species in the above mentioned mechanism is a fundamental step in the exchange process [11]. For pure ionic conductors therefore, the oxygen reduction reaction may be limited due to the lack of electronic species which restricts the catalytic activity, leading to reduced surface exchange rates. One potential solution is to use a humidified

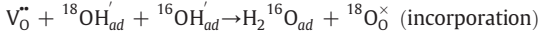
* Corresponding author. Tel.: +44 20 7594 6782; fax: +44 20 7594 6757.

E-mail address: s.skinner@imperial.ac.uk (S.J. Skinner).

atmosphere for the measurement of surface exchange rates as dissociation of water vapor is more facile than the oxygen reduction at the surface and therefore enhances the exchange process. The surface exchange reactions for this case are believed to be as follows [12].



(formation of hydroxyl groups bonded to the cations in the lattice)



A humidified atmosphere is therefore applied when the oxygen isotopic exchange and diffusion measurements are used for pure ionic conductors. However, there are few studies that have focused on the differences between the dry and humidified exchange atmospheres.

For this work, a silver surface coating was introduced because it has been shown to be effective in improving the oxygen dissociation at the surface [13]. Using this method, the oxygen diffusion profiles within $\text{La}_2\text{Mo}_2\text{O}_9$ for different temperatures in a dry $^{18}\text{O}_2$ atmosphere and a H_2^{18}O vapor atmosphere were obtained. The resulting oxygen diffusion coefficients from both atmospheres were compared along with the reported data which had been obtained for a water vapor atmosphere [5]. The activation energy for the oxygen diffusion was calculated from an Arrhenius plot of the diffusion coefficients. Finally, the ionic conductivity of the sample was calculated from the measured oxygen transport contribution within the material and it was compared with the conductivity determined from AC impedance measurements.

2. Experimental

$\text{La}_2\text{Mo}_2\text{O}_9$ powder was prepared by conventional solid state synthesis using La_2O_3 (99.9%, Aldrich) and MoO_3 (99.5%, Aldrich) at 900 °C. Pellets were prepared by cold uni-axial and iso-static pressing and sintered at 1100 °C for 6 h to achieve a high relative density of >95%. X-ray diffraction (XRD) was used to confirm that there was no presence of impurities within the detection limit of the technique. The $\text{La}_2\text{Mo}_2\text{O}_9$ pellets were then polished using diamond suspensions of different grades to a finish of 0.25 μm in order to obtain a shiny flat surface for oxygen isotopic exchange. The samples for dry exchange were then coated with silver (~100 nm) using an Emitech K575X Sputter Coater [13].

For the dry exchange, the sample was pre-annealed in research grade oxygen (99.9996%, BOC Industrial Gases, UK) with a natural isotopic abundance for a duration of 10 times that of the isotopic exchange time for chemical equilibration, thereby removing the surface damage caused by the polishing process. The sample was then annealed in an ^{18}O enriched gas (Isotec Inc. USA) at a pressure of 200 mbar for 30 min at each temperature. In this case the exchange environment is not exposed to the atmosphere and is regularly baked to remove any adsorbed species on the exchange rig. Typical water contents of ~2 ppm have been determined for this rig [14]. For the wet exchange, the water reservoir was kept in a water bath in order to obtain $P_{\text{H}_2\text{O}}$ of 60 mbar. The $^{16}\text{O}_2$ gas at a pressure of 200 mbar was used as the carrying medium. After pre-annealing, the sample was further annealed for the oxygen exchange in isotopically labeled water (H_2^{18}O) (Isotec Inc. USA) by changing to another water reservoir. After the exchange, the water bath was replaced by a liquid nitrogen container to recover the H_2^{18}O vapor. The water reservoir was kept in nitrogen vapor above the liquid level to avoid the condensation of the O_2 carrying gas. Full details of the apparatus for dry and wet exchange are described in previous publications [8,15]. Quick heating and quenching were applied in both exchange methods to

avoid any experimental artifacts (such as an elongated diffusion tail introduced by slow cooling which could be misunderstood as a grain boundary effect). The oxygen isotope compositions of the $^{18}\text{O}_2$ gas and H_2^{18}O vapor respectively were determined by oxidizing a silicon wafer in their respective atmospheres at 1000 °C for 6 h. This was then followed by oxygen isotope measurements using SIMS to acquire the ^{18}O fraction.

After the isotope exchange, the oxygen penetration was determined using SIMS. There are two methods typically used for obtaining an oxygen penetration depth profile and these have been described in detail elsewhere [7,13]. The two SIMS instruments used in this work were an Atomika 6500 with nitrogen primary ion beam (Department of Materials, Imperial College London) and an Atomika 4500 with Ar^+ primary ion beam (Department of Physics, University of Warwick). The incident beam energy on the Atomika 6500 was 5 keV with a measured ion current of 60 nA while on Atomika 4500, an energy of 2.5 keV and 75 nA ion current was used. The beam size was between 20 μm and 30 μm on both instruments which was an acceptable size to measure the diffusion profiles of more than 200 μm . For the samples exchanged at low temperatures and where the diffusion length was between 50 to 100 μm , the beam size on the Atomika 6500 was adjusted to approximately 8 μm to minimize any errors that may be introduced by the relatively low lateral resolution. The use of a coincident low energy electron beam was necessary during profiling to overcome surface charging which is common for electronically insulating materials [16].

The ^{18}O isotopic fraction was calculated directly from the measured secondary ion intensities where:

$$C(x) = \frac{{}^{18}\text{C}}{{}^{18}\text{C} + {}^{16}\text{C}} = \frac{I(^{18}\text{O})}{I(^{18}\text{O}) + I(^{16}\text{O})} \quad (1)$$

in which $I(^{18}\text{O})$ and $I(^{16}\text{O})$ are the measured ion intensities from the SIMS. The isotopic fraction is then normalized to the gas concentration by:

$$C_1(x) = \frac{C(x) - C_{bg}}{C_g - C_{bg}} \quad (2)$$

in which C_{bg} is the background isotopic fraction in the material and C_g the gas concentration. The bulk oxygen diffusion coefficient D^* and surface exchange coefficient k can be obtained by fitting the profile to Crank's solution to Fick's second law of diffusion into a semi-infinite medium [6]. The solution is given as:

$$C_1(x) = \text{erfc}\left(\frac{x}{2\sqrt{D^*t}}\right) - e^{(hx + h^2 D^* t)} \text{erfc}\left\{\left(\frac{x}{2\sqrt{D^*t}}\right) + (h\sqrt{D^*t})\right\} \quad (3)$$

where t is the isotopic exchange time and h is the ratio of k to D^* .

AC impedance measurements were used to obtain the electrical conductivity of $\text{La}_2\text{Mo}_2\text{O}_9$, and study the correlation between the oxygen transport and the materials' electrochemical properties [17]. The instrument used for this was a Solartron 1260 impedance analyzer. Pt electrodes were deposited and sintered at 900 °C for 1 h. Contacts were achieved through Pt mesh current collectors. The samples were measured within the temperature range of 350 °C to 700 °C in air and the frequency range of 0.1 Hz to 13 MHz.

3. Results

Table 1 shows the oxygen isotope exchange experimental details used for this work. The exchange time used varied for different exchange temperatures in order to tailor the length of the diffusion profile so that it was sufficient for the line scan measurement.

The diffusion profiles of isotopically exchanged samples using the dry atmosphere, $^{18}\text{O}_2$ gas, are displayed in Fig.1 (a). Diffusion profiles

for all the temperatures were well fitted using the Crank solution without any additional tailing function [13]. Although the exchange time was varied slightly for each temperature, it is clear that the oxygen transport within the sample experienced a dramatic increase after the phase transition which occurs at ~580 °C. The oxygen diffusion and surface exchange coefficients determined are listed in Table 1.

When the isotope exchange atmosphere was changed to isotopically labeled water (H₂¹⁸O) vapor, the diffusion profiles appear to be similar in form to the profiles obtained in dry atmosphere, with all profiles again showing good fits to the Crank solution, as shown in Fig. 1 (b). In a previous publication [13], a difference between the diffusion profiles obtained for the dry exchange to those previously published for a humidified atmosphere was found whereby it was postulated that a fast grain boundary diffusion path was the possible reason for this difference. In this work, the good fits to Crank's solution to Fick's diffusion law obtained for a wet atmosphere imply that there was no grain boundary tailing for the prepared La₂Mo₂O₉, regardless of exchange atmosphere adopted. The surface isotopic fraction measured for each temperature in the wet atmosphere is much higher than that in the dry exchange at the corresponding temperature [15]. This may be because of rapid dissociation of H₂¹⁸O and incorporation of the oxide species at the surface for the wet atmosphere which is further substantiated by the high surface exchange coefficients found and presented in Table 1.

For oxygen isotope exchange and diffusion measurements, the shape of the diffusion profile offers a reliable way of substantiating the reliability of the derived D^* and k values. Fast diffusion in some oxygen ionic conductors can contribute to a long flat oxygen penetration profile, which is problematic when trying to estimate both D^* and k . However, if the surface ¹⁸O fraction, calculated from Eq. (1), is close to the isotopic gas concentration, this may lead to a low confidence in the obtained surface exchange coefficients [18]. Ideally, the surface ¹⁸O fraction should be around 0.5 in order to keep the estimated D^* and k within the reliable region [15]. A dimensionless parameter $h' = k(t/D)^{0.5}$ is normally introduced to indicate the level of confidence in the calculated D^* and k . If h' is larger than 10, the surface isotopic fraction is approaching 1, which means that the confidence in the obtained k is low. If h' is smaller than 0.1, the surface exchange process is relatively low compared to oxygen diffusion in the bulk. In this case, the confidence in the derived D^* could be reduced. The h' should be adjusted to the region of 0.1–4 to give a diffusion profile which will yield reliable D^* and k . The correlation

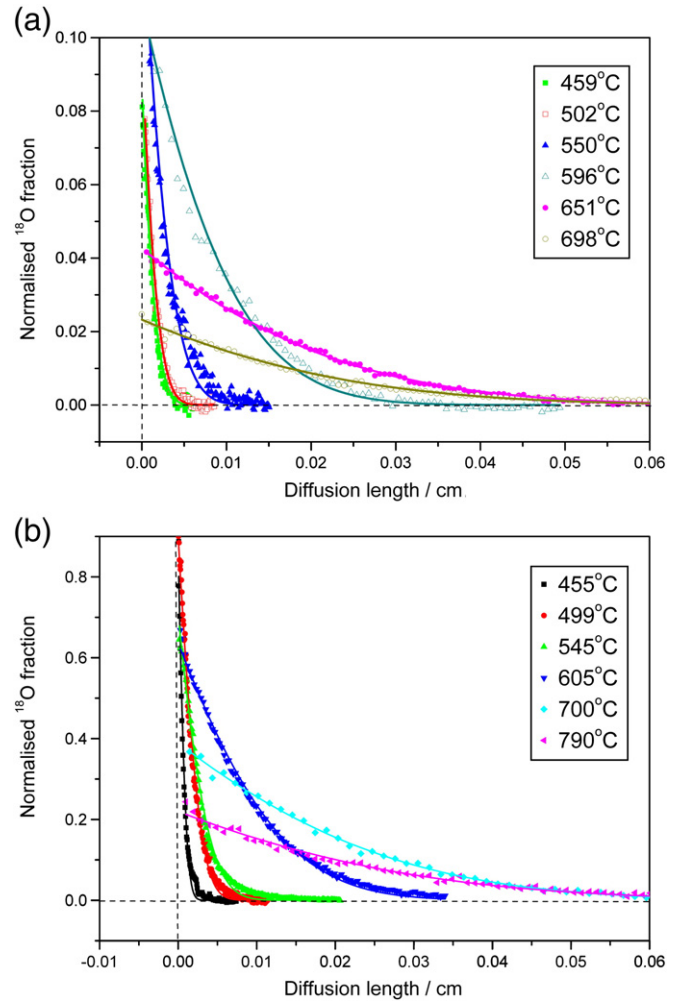


Fig. 1. (a). The diffusion profiles recorded at different temperatures in a dry atmosphere (¹⁸O₂) with the fitting results displayed as solid lines as presented in Ref. [13]. (b). Diffusion profiles recorded at different exchange temperatures in a wet atmosphere (H₂¹⁸O) with the fitting results displayed as solid lines.

between relative surface ¹⁸O fraction and h' parameters calculated from each diffusion profile in both dry and wet exchange is displayed in Fig. 2. The theoretical relationship between these two factors should follow:

$$C_0 = 1 - \exp(-h'^2) \operatorname{erfc}(h') \quad (4)$$

which is derived from Eq. (3) when $x = 0$. As seen in Fig. 2, for the wet exchange most of the data points followed the theoretical line predicted and fell within the region of 0.1–4, meaning that the measured D^* and k are reliable. For the dry exchange, the h' values obtained fell within 0.05–0.15 with a surface ¹⁸O fraction below 0.1, hence the surface exchange is relatively low and the confidence in the obtained D^* is reduced [18].

The Arrhenius plot for the oxygen diffusion coefficients measured from the samples exchanged under dry and wet atmospheres is shown in Fig. 3. The phase transition for both sets of data is clear, with the diffusion coefficient increasing by almost 1.5 orders of magnitude. The oxygen diffusion coefficients for the wet exchange appear to be lower than those for the dry exchange previously presented [13]. For the dry exchange the activation energy in the low temperature monoclinic α phase over the low temperature range (440–550 °C) is found to be 0.66 (± 0.09) eV while the value for the high temperature cubic β phase over the higher temperature range (550–700 °C) is 1.25

Table 1

Experimental details and result summary determined from La₂Mo₂O₉ samples which were isotopically exchanged in dry and wet atmospheres respectively.

| Exchange temp (°C) | Exchange time (s) | D^* (cm ² s ⁻¹) | k (cm s ⁻¹) | ref |
|--|-------------------|--|--------------------------------|-----------|
| <i>Dry atmosphere (¹⁸O₂ enriched gas) 200 mbar</i> | | | | |
| 447 | 1810 | $4.9 (\pm 0.1) \times 10^{-10}$ | $3.0 (\pm 0.1) \times 10^{-8}$ | [13] |
| 459 | 2400 | $6.1 (\pm 1.3) \times 10^{-10}$ | $3.7 (\pm 1.4) \times 10^{-8}$ | [13] |
| 500 | 1200 | $1.5 (\pm 0.1) \times 10^{-9}$ | $5.2 (\pm 0.5) \times 10^{-8}$ | [13] |
| 502 | 1800 | $1.6 (\pm 0.6) \times 10^{-9}$ | $7.6 (\pm 2.6) \times 10^{-8}$ | [13] |
| 550 | 1200 | $6.1 (\pm 0.1) \times 10^{-9}$ | $2.9 (\pm 0.1) \times 10^{-7}$ | [13] |
| 596 | 1200 | $1.1 (\pm 0.7) \times 10^{-7}$ | $7.5 (\pm 0.6) \times 10^{-7}$ | [13] |
| 651 | 1827 | $2.0 (\pm 0.1) \times 10^{-7}$ | $4.2 (\pm 0.2) \times 10^{-7}$ | [13] |
| 698 | 1800 | $3.0 (\pm 0.9) \times 10^{-7}$ | $6.1 (\pm 3.2) \times 10^{-7}$ | [13] |
| <i>Wet atmosphere (H₂¹⁸O) 60 mbar (with 200 mbar ¹⁶O₂ gas)</i> | | | | |
| 455 | 1700 | $2.1 (\pm 0.2) \times 10^{-10}$ | $6.8 (\pm 5.5) \times 10^{-7}$ | This work |
| 459 | 2280 | $1.3 (\pm 0.2) \times 10^{-9}$ | $3.3 (\pm 0.9) \times 10^{-6}$ | This work |
| 545 | 2130 | $4.6 (\pm 1.2) \times 10^{-9}$ | $2.1 (\pm 0.2) \times 10^{-6}$ | This work |
| 595 | 1800 | $6.7 (\pm 1.7) \times 10^{-8}$ | $1.4 (\pm 0.5) \times 10^{-5}$ | This work |
| 605 | 2100 | $3.9 (\pm 0.5) \times 10^{-8}$ | $5.2 (\pm 1.8) \times 10^{-6}$ | This work |
| 700 | 1800 | $2.3 (\pm 0.4) \times 10^{-7}$ | $1.3 (\pm 0.5) \times 10^{-5}$ | This work |
| 790 | 1217 | $5.1 (\pm 0.1) \times 10^{-7}$ | $5.0 (\pm 0.1) \times 10^{-6}$ | This work |

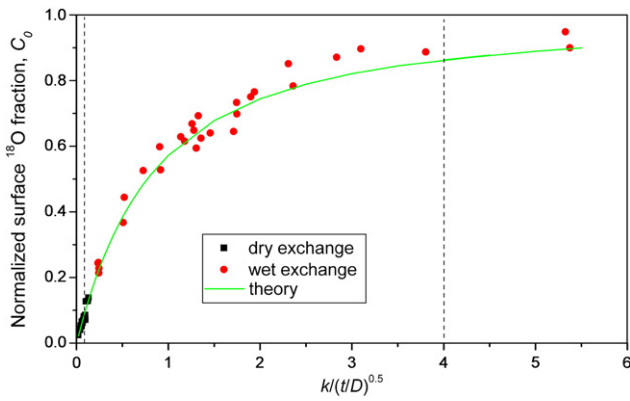


Fig. 2. The normalized surface isotopic fraction, C_0 , as a function of $h' = k(t/D)^{0.5}$. The solid line is the theoretical relationship for diffusion into a semi-infinite specimen and the data points are the starting isotopic fractions in all of the diffusion profiles.

(± 0.01) eV [13]. However, for the wet exchange, the activation energy of oxygen diffusion for the β phase over the high temperature range (550–800 °C) is found to be 0.99 (± 0.18) eV, and the value for the α phase at low temperatures (450–550 °C) is 1.75 (± 0.14) eV. The differences in the diffusion coefficients and the activation energy suggest that the exchange atmosphere has some effect on the oxygen transport properties in $\text{La}_2\text{Mo}_2\text{O}_9$. The results are also compared with the reference data obtained with a wet exchange for $\text{La}_2\text{Mo}_2\text{O}_9$ [5]. Although we observe a decrease in D^* here this may be a result of a chemical difference in the prepared materials because the activation energy (1.11 (± 0.06) eV) for the previously reported data is similar to the wet exchange value of the current work, indicating that there is a difference between dry and wet exchanges.

Fig. 4 presents the surface exchange coefficients from both dry and wet exchanges where the standard deviations are shown in the plot as error bars. It should be noted that for all the samples exchanged in a dry atmosphere the sample surface was coated by a thin (100 nm) silver film to enhance the surface oxygen exchange. Hence, the surface exchange coefficient is a value which indicates the surface property of the $\text{La}_2\text{Mo}_2\text{O}_9$ modified by the silver coating [13]. For the wet exchange, the k values are consistent with those in reference [5]. Due to the large standard deviation it is difficult to obtain reliable activation energies for oxygen surface exchange, but it is likely that the surface exchange process is not affected by the exchange

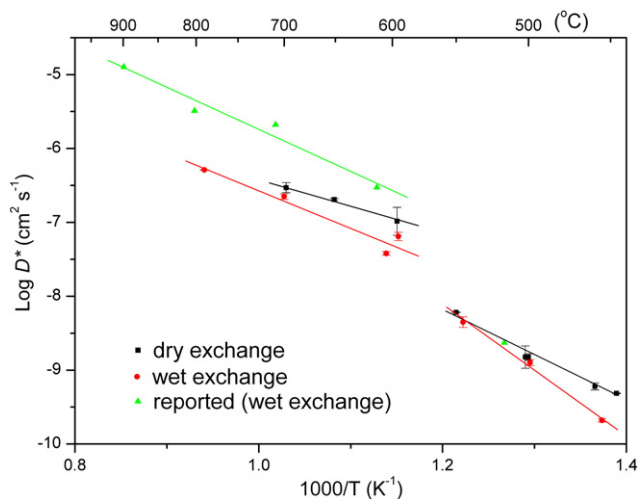


Fig. 3. Arrhenius plot of oxygen diffusion coefficients of $\text{La}_2\text{Mo}_2\text{O}_9$ measured in dry ($^{18}\text{O}_2$ gas) and wet (H_2^{18}O vapor) atmosphere respectively, compared with the previously published data [5] which was obtained in wet exchange. (Standard deviations are shown as error bars).

temperature significantly when the material exists as the beta phase because the surface exchange coefficients vary little for both exchange atmospheres. The plot also indicates that the surface exchange is closely related to the exchange conditions since the k values for the wet exchange are an order of magnitude higher than those for the dry exchange.

The oxygen diffusion coefficient (D^*) reflects the rate of oxygen transport in the material while the ionic conductivity (σ_i) indicates the oxygen ion movement. The correlation between the two is brought together in the Nernst–Einstein relation which relates ion diffusivity and mobility by [16]:

$$D_i = \left(\frac{kT}{q_i} \right) \mu_i, \quad (5)$$

where k is Boltzman constant; q_i is the particle charge; μ_i is electrical mobility. The conductivity can be expressed in terms of charge carrier concentration c_i and mobility μ_i , $\sigma_i = c_i \mu_i q_i$. Therefore, the correlation between diffusivity and conductivity is given by:

$$\sigma_i = \frac{D_{self} \cdot c_i \cdot q_i^2}{kT}. \quad (6)$$

Therefore the oxygen tracer diffusion coefficient measured by the isotope exchange and diffusion measurement can be converted to a self-diffusion coefficient by a correlation factor, f :

$$D^* = f \cdot D_{self} \quad (7)$$

in which the geometrical correlation factor (f) for β - $\text{La}_2\text{Mo}_2\text{O}_9$, which has a primitive cubic structure, is 0.653 [19] while the geometrical correlation factor for α - $\text{La}_2\text{Mo}_2\text{O}_9$ with a monoclinic structure is estimated to be 0.66 [20]. Rigorously the correlation factor should be considered as $f_1 = f + C \cdot g$ where f_1 = physical correlation factor, C = concentration of atoms and g = two particle correlation function [21], but in many cases where the defect concentrations are low the factor $f_1 = f$ [21] can be assumed. It is believed that in this case the defect concentration is low and hence only the geometrical correlation factor is used. Because $\text{La}_2\text{Mo}_2\text{O}_9$ is predominantly an ionic conductor [22], the electrical conductivity determined from AC impedance spectroscopy is

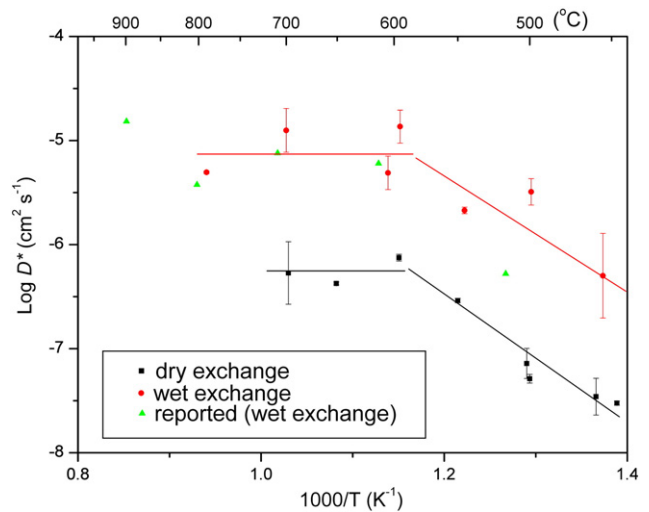


Fig. 4. Arrhenius plot of oxygen surface exchange coefficients of $\text{La}_2\text{Mo}_2\text{O}_9$ measured in dry ($^{18}\text{O}_2$ gas) and wet (H_2^{18}O vapor) atmospheres respectively, compared with the previously published data [5] which was obtained in wet exchange. (Standard deviations are shown as error bars; lines are only shown to reflect the trends).

ionic conductivity. Therefore, the correlation between D^* and σ_i in $\text{La}_2\text{Mo}_2\text{O}_9$ is given by:

$$\sigma_i = \frac{D^* \cdot c_i \cdot q_i^2}{f \cdot k \cdot T} \quad (8)$$

From this relation the charge carrier concentration in the lattice structure can be estimated. Fig. 5(a) compares the conductivity determined from the AC impedance measurements recorded in static air (nominally 'dry') and the calculated value of ionic conductivity determined from measured oxygen diffusion coefficients. Note that the bulk conductivity is used instead of the total conductivity because the diffusion is mainly from the contribution of bulk diffusion. The charge carrier concentration is estimated to be 5, close to the number (4.6) of oxygen ions on the O3 site in the $\text{La}_2\text{Mo}_2\text{O}_9$ structure [23]. There may also be contributions from the oxygen ions on O2 sites because in $\text{La}_2\text{Mo}_2\text{O}_9$ all the oxygen ions on O3 sites are thought to contribute to oxygen ion transport while some of the oxygen ions on O2 sites may also contribute to the total ionic conductivity [24]. As a humidified atmosphere had been used for the wet exchange the effect of this atmosphere on the conductivity data determined from impedance spectroscopy was investigated under an atmosphere of 30 mbar H_2O , Fig. 5(b), from which it is evident that no protonic conductivity could be assigned. Indeed a small decrease in the total

conductivity was observed which may be attributed to grain boundary effects, but further investigation of this phenomenon is required. It is also clear that the determined conductivity values agree well with those calculated from the diffusion coefficients.

4. Discussion

From what has been presented above, there is evidence to indicate a difference for the oxygen transport properties within $\text{La}_2\text{Mo}_2\text{O}_9$ under dry and wet exchange atmospheres. The advantage of a dry exchange over the wet exchange is that in an $^{18}\text{O}_2$ exchange atmosphere there are no other species which could be incorporated that will affect oxygen transport. The silver coating is believed to have no effect on the oxygen diffusion within the bulk [13]. However, due to the instability of silver at temperatures above 700 °C, the maximum exchange temperature is somewhat limited. Wet exchange in a H_2^{18}O vapor has been shown to improve surface oxygen dissociation and incorporation therefore it is typically employed in the isotope exchange and diffusion measurements (especially on electrolyte materials) to overcome the low surface exchange coefficient. However, the observation of a small decrease of oxygen diffusion coefficient and the increased activation energy for the wet atmosphere implies that the humidified environment has some effects on oxygen exchange and diffusion measurement. Therefore the advantages and disadvantages of each exchange method along with the confidence level in obtained D^* and k from the different exchange methods need to be carefully considered.

In regard to the decrease for the oxygen diffusion coefficient using the wet exchange, one possible explanation is the incorporation of hydroxyl species within the bulk [25], which would decrease the number of available positions for oxygen transport. A similar decrease in diffusion coefficient for a humidified atmosphere has been observed in yttrium stabilized zirconia (YSZ) [12]. It was proposed that the hydroxyl species were generated during the surface oxygen dissociation step and could exist stably at the surface of the material. Although whether the incorporated hydroxide species can diffuse into the bulk is not very clear, this assumption is a likely reason to explain the decreased diffusion coefficient in wet exchange. The incorporated hydroxyl species at the surface occupy some oxygen vacancies, leading to fewer available positions for oxygen transport. Therefore, the diffusion coefficient is decreased and the activation energy is increased in wet exchange. Further work is under way to investigate the movement of hydroxyl species in a humidified atmosphere in $\text{La}_2\text{Mo}_2\text{O}_9$.

It is difficult to accurately quantify the obtained surface exchange coefficient due to the large standard deviation. However, it appears that the surface exchange coefficients follow the same trend under both of the exchange conditions. For an exchange temperature below the phase transition point at 580 °C the surface exchange coefficients are temperature dependent. Although the surface oxygen exchange was enhanced for the wet exchange process, the activation energy of the surface exchange and incorporation process is approximately the same for both exchange methods, implying that the exchange environment does not have a significant effect while the oxygen surface incorporation is closely related to the defect mechanism of the electrolyte [26]. When the exchange temperature is increased and the material transits to $\beta\text{-La}_2\text{Mo}_2\text{O}_9$, the activation energy of the surface exchange is greatly reduced and the k values seem to become independent of temperature. Although the surface exchange mechanism is complicated by the number of reactions involved in the process, the lower temperature-dependence of k may indicate at this stage that the oxygen adsorption and dissociation are keys to the surface exchange which could be due to a physical limitation at the surface *i.e.* adsorption sites. Further investigation is required to study the oxygen surface exchange process on $\text{La}_2\text{Mo}_2\text{O}_9$, especially the effects of surface defect mechanism for the alpha and beta phases respectively.

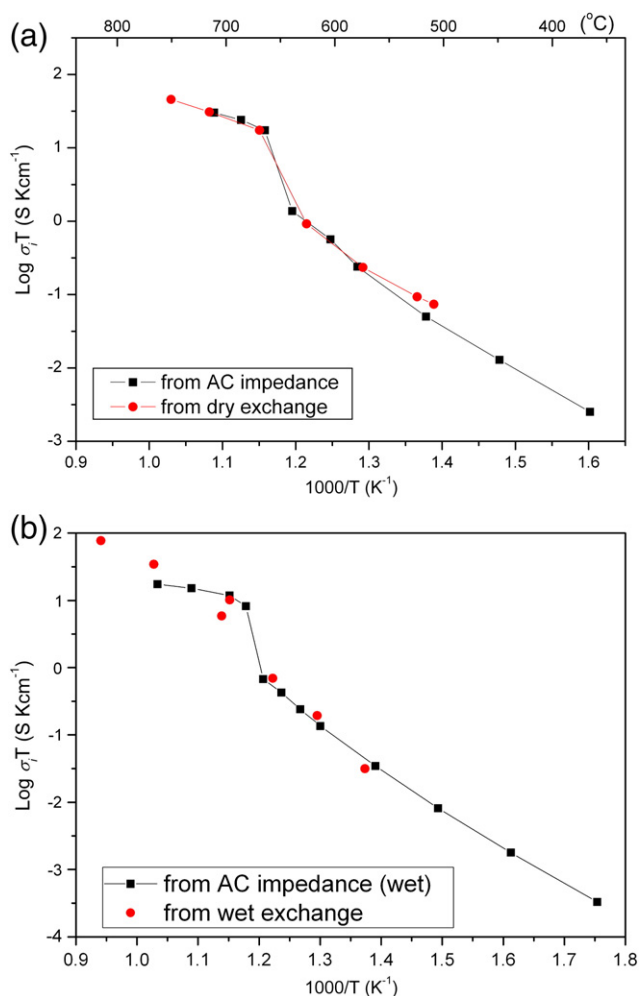


Fig. 5. Correlation between the oxygen diffusion coefficient (a) for the dry exchange data and the measured bulk ionic conductivity in static laboratory air for $\text{La}_2\text{Mo}_2\text{O}_9$ and (b) for wet exchange data and conductivity data measured under a humidified atmosphere where both conductivity data sets were determined from AC impedance spectroscopy.

5. Conclusion

Oxygen isotope exchange and diffusion was carried out on $\text{La}_2\text{Mo}_2\text{O}_9$ using different atmospheres, dry ($^{18}\text{O}_2$) and wet (H_2^{18}O). The oxygen diffusion profiles for both atmospheres did not show any evidence of fast grain boundary diffusion paths, contrary to previously reported data [5]. The surface exchange process was dramatically improved for the wet exchange but the obtained D^* was lower than the value obtained using the dry exchange. In case of the activation energies for the oxygen diffusion, a slightly higher value was found for the wet exchange. It has been proposed that this may be a consequence of using water vapor because this may lead to the incorporation of hydroxyl species which reduce the number of available oxygen positions which in turn results in a decrease in the diffusion coefficient. Further investigation is suggested to confirm this. Interestingly, the surface exchange coefficient (k) exhibited a trend where the values became independent of temperature at $>580^\circ\text{C}$. This suggests that a different rate limiting step could be dominating the surface exchange process. Further investigation is required to understand the rate-limiting factors of the electrolyte surface in respect to oxygen isotope exchange for $\text{La}_2\text{Mo}_2\text{O}_9$ -based materials. By correlating the oxygen diffusion coefficient and ionic conductivity from AC impedance measurement, the concentration of oxygen charge carriers (O^{2-}) was estimated with the number of mobile oxygen ions being 5 per unit cell in $\text{La}_2\text{Mo}_2\text{O}_9$ which is consistent with the structural studies [22].

Acknowledgment

The studentship (J. Liu) funded by the Lee Family Scholarship at Imperial College London, is gratefully acknowledged.

References

- [1] P. Lacorre, F. Goutenoire, O. Bohnke, *Nature* 404 (2000) 856–858.
- [2] S. Georges, F. Goutenoire, P. Lacorre, M.C. Steil, *J. Euro. Ceram. Soc.* 25 (16) (2005) 3619–3627.
- [3] S. Georges, F. Goutenoire, F. Altorfer, D. Sheptyakov, F. Fauth, E. Suard, P. Lacorre, *Solid State Ionics* 161 (3–4) (2003) 231–241.
- [4] S. Georges, F. Goutenoire, Y. Lalignant, P. Lacorre, *J. Mater. Chem.* 13 (9) (2003) 2317–2321.
- [5] S. Georges, S.J. Skinner, P. Lacorre, M.C. Steil, *Dalton Trans.* 19 (2004) 3101–3105.
- [6] J.A. Kilner, B.C.H. Steele, *Solid State Ionics* 12 (1984) 89–97.
- [7] R.J. Chater, S. Carter, J.A. Kilner, B.C.H. Steele, *Solid State Ionics* 53–56 (1992) 859–867.
- [8] P.S. Manning, J.D. Sirman, J.A. Kilner, *Solid State Ionics* 93 (1997) 125–132.
- [9] J.A. Lane, J.A. Kilner, *Solid State Ionics* 136–137 (2000) 927–932.
- [10] T. Horita, K. Yamaji, N. Sakai, M. Ishikawa, *Electrochem. Solid State Lett.* 1 (1998) 4–6.
- [11] B.A. Boukamp, B.A. Van Hassel, I.C. Vinke, K.J. De Vries, A.J. Burggraaf, *Electrochimica Acta* 38 (14) (1993) 1817–1825.
- [12] N. Sakai, K. Yamaji, T. Horita, *J. Electrochem. Soc.* 150 (2003) A689–A694.
- [13] J. Liu, R.J. Chater, B. Hagenhoff, R.J.H. Morris, S.J. Skinner, *Solid State Ionics* 181 (2010) 812–818.
- [14] R.N. Vannier, *Solid State Ionics* 160 (2003) 85–92.
- [15] A. Atkinson, R.J. Chater, R. Rudkin, *Solid State Ionics* 139 (2001) 233–240.
- [16] B. Guzmán de la Mata, M.G. Dowsett, R.J.H. Morris, *J. Vac. Sci. Technol. A24* (4) (2006) 953–956.
- [17] Y.M. Chiang, D.P. Birnie, W.D. Kingery, *Physical Ceramics: Principles for Ceramic Science and Engineering*, Chichester: John Wiley, New York, 1997.
- [18] J.A. Kilner, R.A. De Souza, *International Symposium on Materials Science: High Temperature Electrochemistry—Ceramics and Metals*, 1996, Denmark.
- [19] P.G. Shewmon, *Diffusion in Solids*, 2nd ed., Minerals, Metals & Materials Society, Warrendale, 1989.
- [20] J.N. Sherwood, *The Plastically Crystalline State*, Wiley, London, 1981.
- [21] S.A. Akbar, *J. Appl. Phys.* 75 (1994) 2851–2856.
- [22] D. Marrero-López, J.C. Ruiz-Morales, D. Pérez-Coll, P. Núñez, J.C.C. Abrantes, J.R. Frade, *J. Solid State Electrochem.* 8 (9) (2004) 638–643.
- [23] F. Goutenoire, O. Isnard, E. Suard, *J. Mater. Chem.* 11 (2001) 119–124.
- [24] P. Lacorre, A. Selmi, G. Corbel, B. Boulard, *Inorganic Chem.* 45 (2) (2006) 627–635.
- [25] Liu J., Chater R. J., Skinner S. J., *Solid State Ionics*, in press (doi:10.1016/j.ssi.2010.03.021).
- [26] T. Ramos, A. Atkinson, *Solid State Ionics* 170 (2004) 275–286.